

Low Pass Filter with Hybrid Fuzzy Design for Balancing the Two-Wheeled Mobile Robot Application

M. T. Abdul Rahman, Salmiah Ahmad, and Rini Akmeliawati Department of Mechatronics Engineering, International Islamic University Malaysia, Malaysia

Abstract—This paper proposes a low pass filter and hybrid fuzzy design for balancing an extendable double-link two-wheel mobile robot (TWMR) system. The proposed system mimics a double inverted pendulum scenario, where the angular position of the first link (Link1) is to be varied depending on the value of the angular position of the second link (Link2) and the elongation of the extendable link (Link3) attached to Link2 and with various payloads. The two-wheeled mobile robot together with the extendable link on Link2 makes the system become more flexible but yet unstable without any controller. The inclination of the Link3 at any interest angle of Link2 will affect the centre of gravity (COG) of the system especially when the payload is having a significant weight. Although, the system can be balanced by controlling the COG analysis via the hybrid fuzzy controller, but the responses are still oscillating and not smooth. Thus, an additional low pass filter is designed and added to shape the controller outputs, before the signals are fed into the TWMR system. The results obtained show that the filter designed managed to improve the oscillating and smoothing of the angular position of Link1 and Link2 within a shorter time. The performance of the system, such as the settling time and the rise time of the responses are improved by at least 43%. Meanwhile, the root mean square error of the responses can be improved up to 60.7%.

Keywords—TWMR, intelligent controller, double inverted pendulum, low pass filter.

I. INTRODUCTION

TWO-WHEELED robot has its own vital trait in moving itself at one position at a very less turning radius that allows it to run within its restricted area [1]. In a way that the system's balancing concept is performed through the movement of the center of gravity of the vertical axis, i.e. along the wheel's vertical axis so that it will always be at the upright position [2]. As concurrent to the investigation made by most of the researchers, the manipulator controls through center of gravity approaches are obtained as such [3], [4], and [5]. Those approaches keen to benefit the smooth trajectory of the COG upon taking the stability of the COG into consideration. In controlling the two-wheeled robot, there are many approaches that can simply be classified into two different methods, the

Corresponding author: R. Akmeliawati (e-mail: rakmelia@iium.edu.my). This paper was submitted on February 28, 2014; revised on November 20, 2014; and accepted on November 25, 2014.

first one considering the mobile robot as a separate part; manipulator and wheels, and has two control systems each. Secondly, the manipulator part and wheel are to be considered as one system of mobile robot [6]. The latest research on COG analysis is on an extendable double-link system on two-wheel mobile robot (TWMR) and founds that the result that representing the stabilization of the system is merely unstable. Eventually this produces unsmooth trajectories results and upon that required some filters to eliminate noises [7]. In this paper, we opt to apply low pass filter in order to encounter the problem. Low pass filter is amongst the continuous-time (CT) filter category. CT filter has better privilege compared to Discreet Time Filter whereby the visual aspect of CT Filter produces better results as it involves in Analog-to-Digital and Digital-to-Analog (ADC-DAC) converters that are applied Digital Signal Processing (DSP) solutions. CT filter could also be applied for anti-aliasing function they can also be used for smoothing purposes at the output of DAC's [8]. As we are considering a smoother output signal, thus we are using low pass filter [9] to overcome the unwanted noise on the TWMR system output signal.

The present work is concerned with the design of a low pass filter that affects the value of the angular position of Link1 and Link2. The paper is organized as follows. The introduction of COG analysis, with the design of the controller and low pass filter, are presented in Section II. Some simulation results are included in Section III. Finally, the concluding remarks are stated in Section IV.

II. CENTER OF GRAVITY (COG) ANALYSIS

A. Location of COG

The COG of the entire system is found as the resultant of the COG of individual manipulator. [10]. Referring to the **Figure 1**, the representing the location of COG of varying angle of a) the COG of angle of Link2, θ_2 and b) the COG of the system that is moved to the upright after manipulating angle of Link1, θ_1 . Basically, to determine the exact location of COG is through the centre of origin, O that accumulates all the respective payloads, R_i with each link's unit vectors, \hat{u}_i in terms of its manipulation values, as referred below [11],

$$\hat{R}_{COG} = R_1 \hat{u}_1 + R_2 \hat{u}_2$$

$$\hat{u}_1 = \sin \theta_1 \hat{i} + \cos \theta_1 \hat{j}$$

$$\hat{u}_2 = \sin(\theta_1 + \theta_2) \hat{i} + \cos(\theta_1 + \theta_2) \hat{j}$$

$$R_1 = (M_1 L_{cog1}) / M_{total}$$

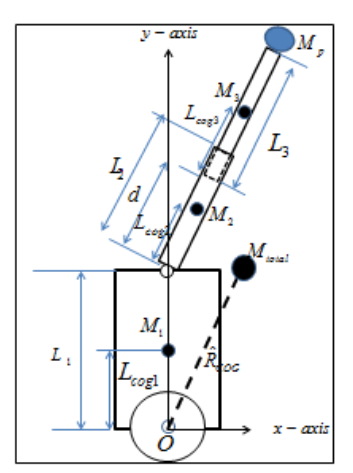
$$R_2 = (M_2 L_{cog2} + M_3 L_{cog3} + M_3 d + M_p L_3) / M_{total}$$

As related to the previous formulas, when \hat{u}_1 , \hat{u}_2 , R_1 and R_2 are added to **Equation 1** and put in the form of $\hat{\iota}$ and $\hat{\jmath}$, obtain the following formula

$$\hat{R}_{COG} = [R_1 \sin \theta_1 + R_2 \sin(\theta_1 + \theta_2)]\hat{i}$$

$$+ [R_1 \cos \theta_1 + R_2 \cos(\theta_1 + \theta_2)]\hat{j}$$
(2)

where based on the below figure, M_1 , M_2 and M_3 correspond to the mass of Link1, Link2 and extendable-link, accordingly, while, the length of Link1, Link2 and Link3 are represented by L_1 , L_2 and L_3 . From the figure, the exact location of center of mass of every each of the links is labeled as L_{COG1} , L_{COG2} and L_{COG3} , in terms \hat{u}_i . It is in the state of real and imaginary of θ_1 and θ_2 . Whereby R_1 is a constant value of, L_{COG1} and M_{total} and R_2 is a function of constants (M_2 , M_3 , L_2 , L_3 , L_{COG2} and L_{COG3}). The manipulated value of displacement of the extendable-link, d is fixed to be 0.1 m.



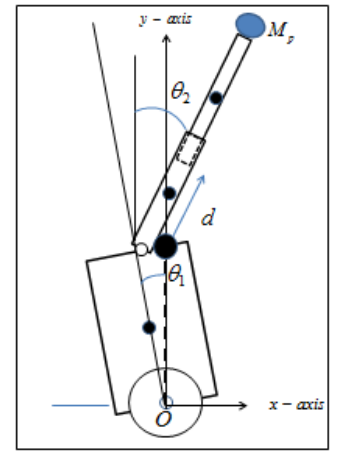


Figure 1 a. COG location

b. COG at upright position

By considering Link1's reference position that must be at the most upright position, thus zero value is set for its initial value θ_I obtaining as the following formula:

$$\hat{R}_{COG} = [R_2 \sin(\theta_2)]\hat{i} + [R_1 + R_2 \cos(\theta_1)]\hat{j}$$
(3)

Inverse of trigonometric function method is applied in order to obtain the angular position of COG as below:

$$\theta_{cog} = 90 - \arctan\left(\frac{R_1 + R_2 \cos(\theta_1)}{R_2 \sin(\theta_2)}\right) \tag{4}$$

Table I below shows all the required parameters used where the system can be considered operating in static condition of a manipulator.

TABLE I SYSTEM'S PARAMETERS

Parameter	Value
M_1	0.900kg
M_2	0.075kg
M_3	0.075m
L_{I}	0.200m
L_2	0.150m
L_3	0.170m
L_{cog1}	0.100m
L_{cog2}	0.075m
L_{cos3}	0.085m
D	0.100m

B. The COG-based angular position of the mobile robot

We shall elaborate further in this part on the method of center of gravity-based position control over the manipulator and the payload so as to stabilize the system. In order to control the angular position based on the COG so that the manipulator system is stable and to avoid it falling, the COG on the imaginary vertical line of the particular wheel is adjusted from the position of the manipulator where we acknowledged it as angular position of Link1 (θ_1) to stabilize the system [12]. Eventually, we can observe that the wheels will shift ahead and rearward to adhere with the changes made by COG. Through the equations obtained, both of the position and the COG of the manipulator are absolutely being controlled as what has been recommended by the COG control method. The following **Figure 2** illustrates the system block diagram and also the controller implemented in this paper.

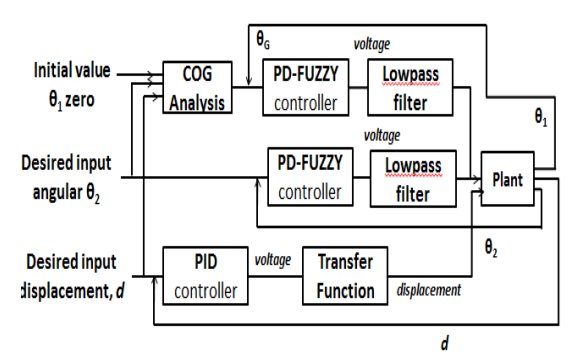


Figure 2 PD-Fuzzy System Block Diagram

The modular hybrid control implemented is illustrated in **Figure 3** that used of fuzzy-PD type discussed in [13], which overall has the control over the angular position of Link1 and Link2. The PID controller was implemented for the extension of the extendable link. Fuzzy Logic Controllers (FLCs) are based on Proportional-Derivative (PD) type where the inputs are the error (e) and change of error (Δe) while the outputs for both FLCs are voltage as shown in **Figure 3**.

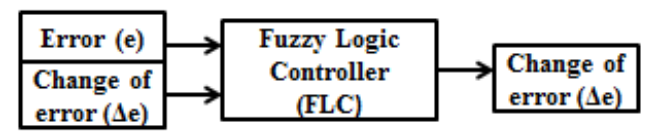


Figure 3 FLC with Two Inputs and One Output

The membership function for fuzzy set of the error (e) and change of error (Δ e) for both Link1 and Link2 controls are; Negative Big (NB), Negative Small (NS), zero (Z), Positive Small (PS) and Positive Big (PB). The relation of membership function between input and output (fuzzy rules) were shown in **TABLE II**. The fuzzy rules are set in the sense that the system is stabilized by moving the wheels forward and backward to achieve the desired angular position of Link2, θ_2 . The Gaussian type membership function type was used in the FLC design.

TABLE II FUZZY RULES MADE FROM MEMBERSHIP FUNCTION OF TWO INPUTS AND ONE OUTPUT

Error ΔError	NB	NS	Z	PS	PB
NB	PB	PB	PB	PS	Z
NS	PB	PB	PS	Z	NS
Z	PB	PS	Z	NS	NB
PS	PS	Z	NS	NB	NB
PB	Z	NS	NB	NB	NB

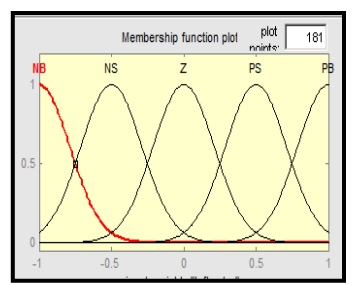
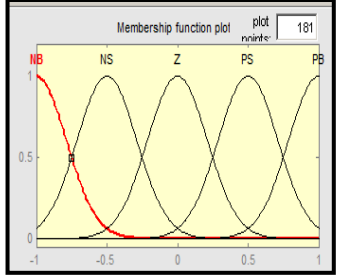


Figure 3 a. Membership Function of error (e)



b. Membership Function of change of error (Δe)

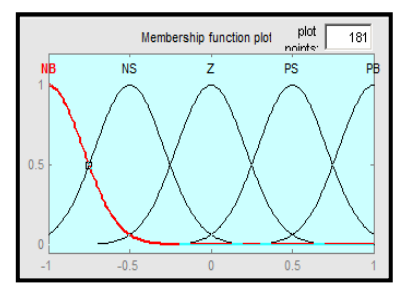


Figure 4 Membership Function of the output (voltage) for left, right and top motors.

The angular position of Link1, θ_I reference input is altered respectively over the angle of the COG of the system to stabilize the whole system. By heuristic tuning, the input gain of the error (e) and the change of error (Δ e) and the output gain of V_L and V_R , the performance of the system can be improved.

Before sending the control output signal to the linear actuator motor, the transfer function was derived for the dynamics of the extendable-link to be used with the PID controller, which at the end it will be converted from voltage displacement condition. Consequently, the length/ displacement are received by linear actuator motor through the simulation. PID controller is used to control the elongation of the linear actuator of the second link. PID controller has historically been considered to be the best controller. The reason PID controllers are so popular is that using PID gives the designer a larger number of options and those options mean that there are more possibilities for changing the dynamics of the system in a way that helps the designer. By tuning the three parameters in the PID controller algorithm, the controller can provide control action designed for specific process requirements. The response of the controller can be described in terms of the responsiveness of the controller to an error, the degree to which the controller overshoots the set point and the degree of system oscillation. Note that the use of the PID algorithm for control does not guarantee optimal control of the system or system stability. The input of PID controller is the value of elongation (0-13cm) where the output is control voltage to linear actuator motor. If the PID controller parameters are chosen incorrectly, the controlled process input can be unstable. In this research, PID parameters are chosen. Instability also caused by wrong excess gain, particularly in the presence of significant lag. So, the gain or coefficient of each parameter should be tuned properly. After several manual tunings of the PID controller, the system's performance becomes stable and balance. TABLE III shows the coefficient of each parameter of PID controller for elongation of linear actuator in second link.

TABLE III COEFFICIENT OF PARAMETER

Parameter	Coefficient		
Proportional (kP)	0.15		
Integral (kI)	0.0009		
Derivative (kD)	0.05		

The transfer function is no need for Link1 and Link2 as the output of PD-Fuzzy controller already in term of velocity. Meanwhile, model for extendable-link will receive orientation of elongation of the link. So, the transfer function should be developed only for extendable-link. The control voltage from the controller for extendable-link will be converted into displacement or elongation (centimeter) so that the simulation motor can read and understand the data send it. Second transfer function is for the linear actuator motor. This transfer function will convert data from voltage to displacement before send it to linear actuator motor.

C. Low pass filter (LPF) design

The ideal filters allow distortion transmission of a certain band of frequencies and completely suppress the remaining frequencies. The ideal LPF is shown in **Figure 5**, allows all components below $\omega = f_C$ rad/s to pass without distortion and suppresses all component above $\omega = f_C$. The ideal LPF has a linear phase of slope, which results in a time delay in seconds

for all its input component of frequencies below $\omega = f_C$. The ideal filter is non-causal and unrealizable, which forms the measure of the practical filters design as shown below.

Continuous-time filters can also be described in terms of the Laplace transform of their impulse response, in a way that lets all characteristics of the filter be easily analyzed by considering the pattern of poles and zeros of the Laplace transform in the complex plane. A typical LPF has a maximum gain at $\omega = 0$. Because a pole enhances the gain at the frequencies in its vicinity, we need to place a pole (or poles) on the real axis opposite to the origin (j ω). The transfer function of low pass filter of this system is described by **Equation 5** [14].

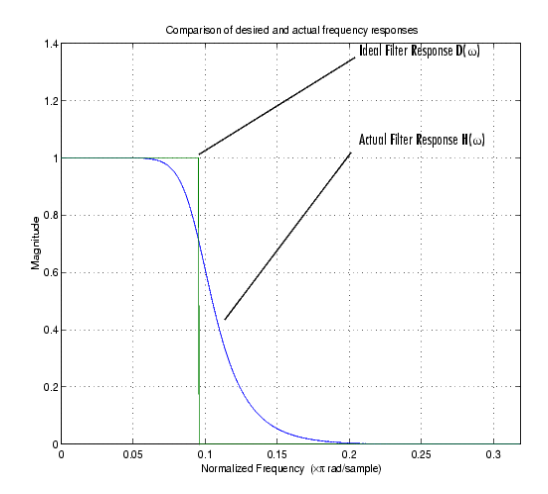


Figure 5 Ideal and actual low pass filter

$$H(s) = \frac{\omega_c}{s + \omega_c} \tag{5}$$

where ω_c is cutoff frequency that is obtained from half time of the value of input signal (voltage) spectrum of Link1 and Link2 through Discrete Fourier-time process as shown in **Figure 6** and **7**. Both figures illustrate the plot of signal spectrum (frequency domain representation), representation of 1000 samples at a sampling rate of 2002 Hz; where we can clearly observe that the amplitude peak is located at the frequency of 500 Hz in the calculated spectrum for Link1 and 996 Hz for Link2. So, the the ω_c for Link1 and Link2 is taken at 250 Hz and 498 Hz respectively.

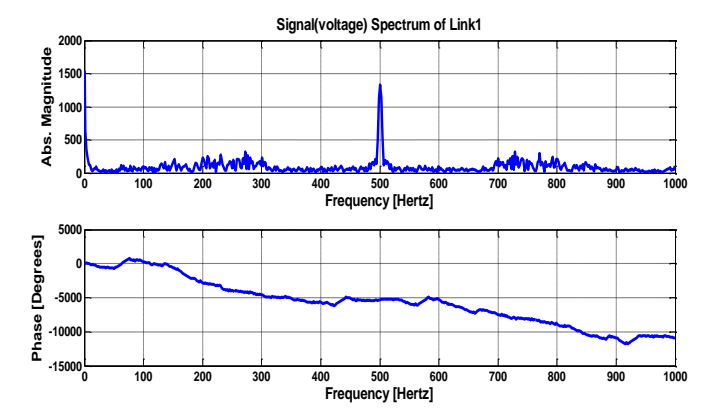


Figure 6 Signal spectrum of Link1

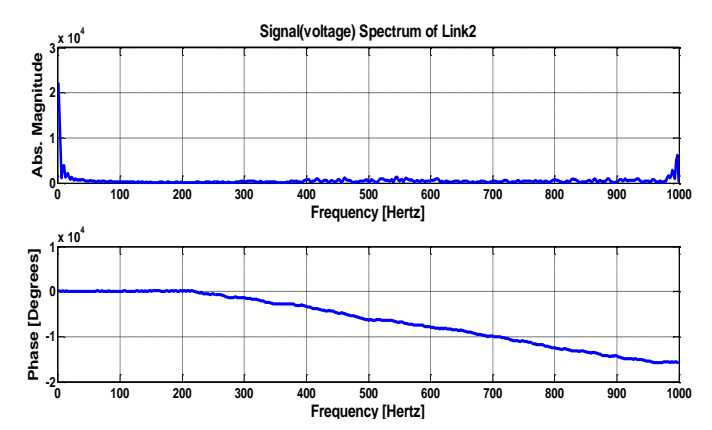


Figure 7 Signal spectrum of Link2

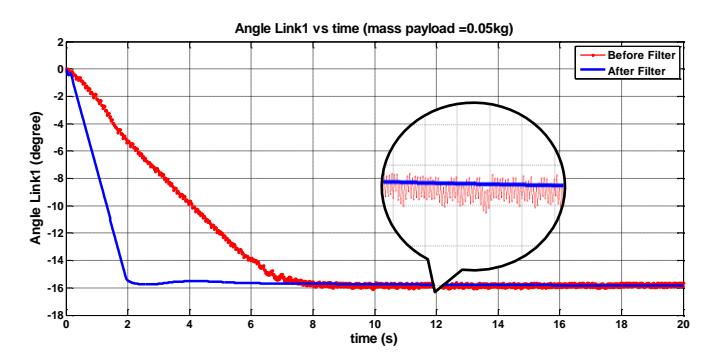


Figure 8 The value of θ_1 = -15.81° and M_p =0.05 kg

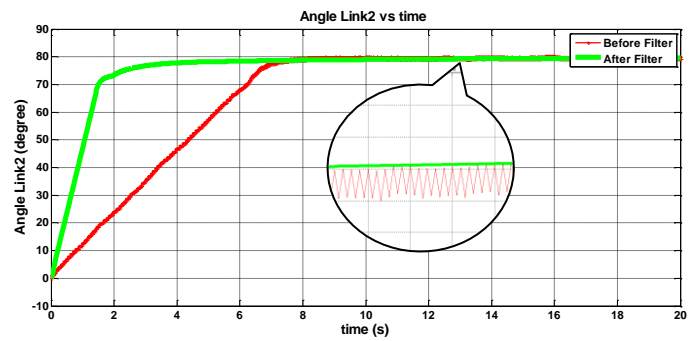


Figure 9 The value of $\theta_2 = 80^{\circ}$ and $M_p = 0.05$ kg

III. SIMULATION RESULTS AND ANALYSIS

A. Figures and Tables

The system has three desired variables which need to be controlled; θ_1 , θ_2 and d. The simulation was conducted by setting the desired angular position of Link2, θ_2 at 80° with constant payload, M_p while maintaining d at 0.1m. We can see from the graphs shown that the variations in θ_1 is depending on θ_{COG} , in the sense that the angular position θ_1 is directly proportional to the value of θ_{COG} to ensure that the position of COG of the system will return back to the upright position.

Figure 8 indicates the angular position of Link1, θ_1 before and after the implementation of the LPF. The figure shows the angle path trajectory before the implementation of the LPF was not smooth. The highest cutoff frequencies will give the best result in term of promptness to achieve the desired target.

Figure 9 shows the comparison between the output value angular position of Link2, θ_2 before and after the implementation of the LPF. From the results we can see that the output performance of both angular position of Link1, θ_1 and the angular position of Link2, θ_2 become smoother and better than before. Based on the result obtained for RMSE before and after filtering for angle Link1, which after filtering obtained is 2.67 while before filter the RMSE of ω was 5.32 (i.e. an improvement of 49%). In addition for Link2, RMSE result of after filtering is 15.73 and before filtering was 40.01 (i.e. an improvement of 60.7%). From the RMSE results shows the average error before and after filtering for both Link1 and Link2, where the average error of Link1 is slightly smaller compared to the average error in Link2 with the difference of 2.65 for average error before and after for Link1 and 24.28 for average error before and after for Link2. The settling times of the response for Link1 and Link2 before and after filtering have been improved by 43%.

The overall results show that the designed modular hybrid controllers integrated with low pass filtering process provides better system performance with smoother system outputs of Link1 and Link2 of the extendable double-link TWMR although there is phase shift during the process. The flexibility of the system was tested by varying θ_2 within the range of [-80°, 80°] via the implementation of intelligent Fuzzy-PD controller. The algorithm is to be applied to the actual hardware of the TWMR in the near future, as can be seen in **Figure 10**.



Figure 10 Extendable double-link TWMR prototype hardware developments

IV. CONCLUDING REMARKS

The COG-based angular position control of an extendable TWMR was integrated with the implementation of the Low Pass Filter. The low pass filter has been designed based on the systems output performance, which was significantly improved after the implementation of the designed LPF. The research made has emphasized smoothing the system outputs by implementing the LPF on the control output signal prior feeding the signals to the system. The multiplication of highest gain of the transfer function of the LPF has helped in achieving the desired value of angular position in shorter time. These

findings will lead to more other future progress on the two wheeled mobile robot.

REFERENCES

- [1] Bin, H., Zhen, L. W., & Feng, L. H. (2010, March). The Kinematics Model of a Two-Wheeled Self-Balancing Autonomous Mobile Robot and Its Simulation. In Computer Engineering and Applications (ICCEA), 2010 Second International Conference on (Vol. 2, pp. 64-68)
- [2] Ghani, N. A., Yatim, N. M., & Azmi, N. A. (2010, October). Comparative assessment for two wheels inverted pendulum mobile robot using robust control. In *Control Automation and Systems (ICCAS)*, 2010 International Conference on (pp. 562-567)
- [3] Stilman, M., Olson, J., & Gloss, W. (2010, May). Golem krang: Dynamically stable humanoid robot for mobile manipulation. In *Robotics and Automation (ICRA)*, 2010 IEEE International Conference on (pp. 3304-3309)
- [4] Abeykoon, A. M. H. S., & Ohnishi, K. (2005, August). Traction force improvement of a two wheel mobile manipulator by changing the centre of gravity. In *Industrial Informatics*, 2005. INDIN'05. 2005 3rd IEEE International Conference on (pp. 756-760)
- [5] Acar, C., & Murakami, T. (2010, March). Motion control of dynamically balanced two-wheeled mobile manipulator through CoG manipulation. In Advanced Motion Control, 2010 11th IEEE International Workshop on (pp. 715-720)
- [6] Larimi, S.R.; Zarafshan, P.; Moosavian, S.A.A. (2013, February). Stabilized Supervising Control of a Two Wheel Mobile Manipulator. In RSIIISM International Conference on Robotics and Mechatronics, 2013.
- [7] Rahman, M. A., Ahmad, S., Akmeliawati, R., Altalmas, T., & Aula, A. (2013, December). Centre of Gravity (COG)-Based Analysis on the Dynamics of the Extendable Double-Link Two-Wheeled Mobile Robot. In *IOP Conference Series: Materials Science and Engineering* (Vol. 53, No. 1, p. 012079). IOP Publishing.
- [8] Tsividis, Y. P. (1994). Integrated continuous-time filter design-an overview. Solid-State Circuits, IEEE Journal of, 29(3), 166-176. CrossRef
- [9] R. K. Lea, R. Allen and S. L.Merry, "A comparative study of control techniques for an underwater flight vehicle," *International Journal of Systems Science*, volume 30, number 9, 1999, pp. 947- 964 <u>CrossRef</u>
- [10] Yang, J. S., & Chang, Y. S. (2005, October). Standing control of a four-link robot. In Systems, Man and Cybernetics, 2005 IEEE International Conference on (Vol. 1, pp. 679-684)
- [11] Fattah, A., & Agrawal, S. K. (2006, May). Gravity-balancing of classes of industrial robots. In Robotics and Automation, 2006. ICRA 2006. Proceedings 2006 IEEE International Conference on (pp. 2872-2877)
- [12] Torige, A., & Ihara, T. (1997, July). Control of manipulator with gravity center position control on mobile vehicle. In Advanced Robotics, 1997. ICAR'97. Proceedings. 8th International Conference on (pp. 367-372)
- [13] Ahmad, S., Aminnuddin, M., & Shukor, M. A. (2012, July). Modular hybrid control for double-link two-wheeled mobile robot. In Computer and Communication Engineering (ICCCE), 2012 International Conference on (pp. 807-813)
- [14] Ambardar, A. (2006). Digital Signal Processing-A Modern Introduction. Thomson-Engineering.
- [15] Lathi, B. P. (2009). Linear systems and signals. Oxford University Press.